

Salinity dependence of ^{226}Ra adsorption on montmorillonite and kaolinite

Shuji Tamamura · Takahiro Takada ·
Junpei Tomita · Seiya Nagao · Keisuke Fukushi ·
Masayoshi Yamamoto

Received: 18 July 2013 / Published online: 8 September 2013
© Akadémiai Kiadó, Budapest, Hungary 2013

Abstract The effect of NaCl concentration (10.0–1,000 mM) on ^{226}Ra adsorption was investigated in the presence of montmorillonite and kaolinite. A positive correlation was observed between the dissolved ^{226}Ra and NaCl concentrations in the presence of these adsorbents. Distribution coefficients decreased from the order of 10^4 to 10^0 (mL g^{-1}) with an increase in NaCl concentration. Although the coefficients were higher for montmorillonite than kaolinite at lower NaCl concentrations, the trend was reversed at higher NaCl concentrations (≥ 500 mM) owing to the sharper reduction of the coefficient for

montmorillonite with the increase in NaCl concentration. The rapid reduction was ascribed to higher negative charge density of montmorillonite, which leads the Ra^{2+} adsorption mechanism to approach charge-compensating ion exchange.

Keywords Radium · Adsorption · Montmorillonite · Kaolinite · Salinity · Distribution coefficient

Introduction

Radium (Ra) is produced from U, Th, and Ac decay series in natural environments, and it has various isotopes with different half-lives: ^{223}Ra (11.4 day), ^{224}Ra (3.66 day), ^{226}Ra (1,599 year), and ^{228}Ra (5.75 year). Owing to the potential risks associated with their radioactivity, their behavior in natural aquifers has attracted considerable attention from the viewpoint of water resource assessments [1–4], risk management for mining workers [5, 6], and safety assessment for the underground disposal of radioactive wastes [7–11].

In natural groundwater, Ra concentrations are often higher in saline aquatic systems [1, 4, 9, 10, 12–16]; various mechanisms have been suggested to explain this phenomenon, such as competitive adsorption of Ra with other cations [1, 10, 12, 14, 16, 17], formation of soluble Ra complexes with Cl^- [8], competitive Ra and Ba incorporation into solid-phase barite [12], ionic-strength-dependent silica reequilibration on quartz grains [12], and dilution by freshwater [13].

The phenomenon of Ra adsorption on aquifer solids was readily manifested by the $^{224}\text{Ra}/^{228}\text{Ra}$ [7, 10, 13] and $^{222}\text{Rn}/^{226}\text{Ra}$ [4] radioactivity ratios in groundwater. Among the adsorbents, clay minerals play an important role owing

S. Tamamura · T. Takada · J. Tomita · S. Nagao ·
M. Yamamoto
Low Level Radioactivity Laboratory, INET, Kanazawa
University, O24, Wake, Nomi, Ishikawa 923-1224, Japan

S. Nagao
e-mail: s_nagao@llrl.ku-unet.ocn.ne.jp

M. Yamamoto
e-mail: pluto@llrl.ku-unet.ocn.ne.jp

Present Address:

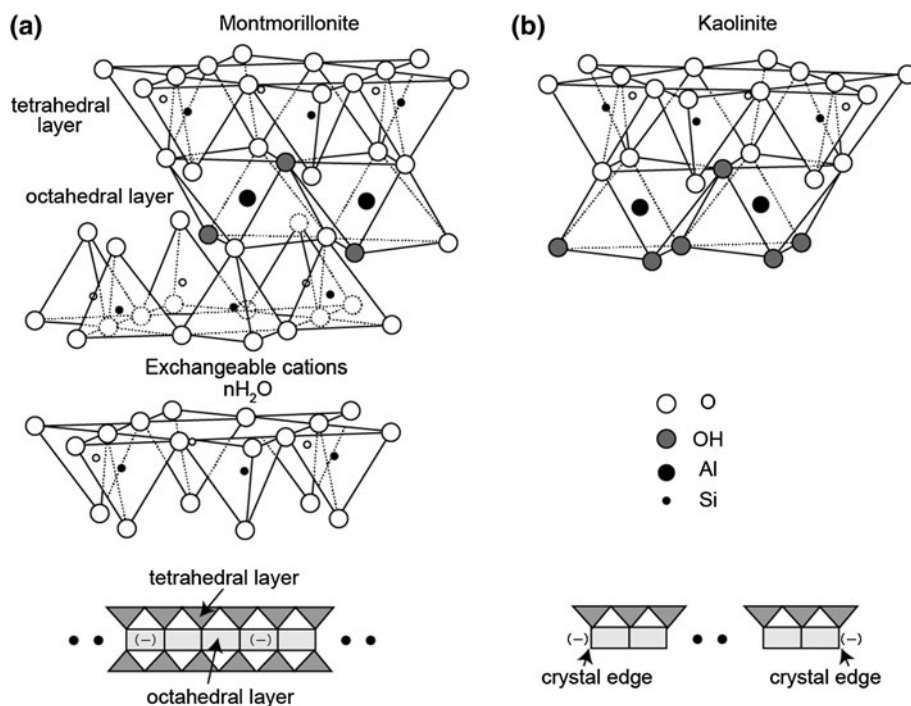
S. Tamamura (✉)
Horonobe Research Institute for the Subsurface Environment,
5-3 Sakae-machi, Horonobe-cho, Teshio-gun,
Hokkaido 098-3221, Japan
e-mail: shuji-tamura@h-rise.jp

Present Address:

J. Tomita
Japan Atomic Energy Agency, 2-4 Shirane, Shirakata, Tokai-
mura, Naka-gun, Ibaraki 319-1195, Japan
e-mail: tomita.jumpei@jaea.go.jp

K. Fukushi
Institute of Nature and Environmental Technology, Kanazawa
University, Kakuma-machi, Kanazawa, Ishikawa 920-1192,
Japan
e-mail: fukushi@staff.kanazawa-u.ac.jp

Fig. 1 Crystal lattice of **a** montmorillonite and **b** kaolinite [18]. The image of negative charge (–) distribution in the crystal structure is illustrated *below* the crystal lattice



to their high cation exchange capacity (CEC) and large specific surface area [18]. The accumulation of Ra in clay minerals during dissolved Ra transportation was consistently indicated by Pb isotopes in clay minerals in the Oklo uranium deposit, central Africa [11].

It has been confirmed via adsorption experiments that Ra has high affinity for clay minerals [5, 19–23]. However, the effect of salinity on the Ra adsorption has not been revealed in relation to crystal structure and CEC of the clay minerals. To understand salinity-dependent Ra concentrations in natural groundwater in terms of clay mineral types in the aquifers, this study focused on the effect of NaCl concentration on Ra adsorption on montmorillonite and kaolinite, which are commonly formed by water–rock interactions [24] yet have different CEC and crystal structures [18, 24].

Experimental

Clay mineral treatment

Wyoming (USA) montmorillonite (SWy-2) and Georgia (USA) kaolinite (KGa-2) were purchased from the Clay Minerals Society (Chantilly, VA, USA). Their structures are illustrated in Fig. 1. Montmorillonite is made of one octahedral layer with both sides fused by Si^{4+} tetrahedral layers (2:1 structure), whereas kaolinite is made of one octahedral layer with only one side fused by a Si^{4+} tetrahedral layer (1:1 structure). In montmorillonite, some Al^{3+} in the octahedral layer is absent or replaced with Mg^{2+} ,

giving a permanent negative charge to the mineral. The negative charges are compensated by ion exchangeable cations intercalated between the layers. At the broken edge of the crystal lattice, ionized surface groups (sianol and aluminol) with net negative charges [18] are exposed. The edge sites are major adsorption sites for kaolinite [18] because kaolinite has a much lesser permanent charge compared to montmorillonite [18].

The exchangeable cations in these clay minerals were saturated with Na^+ via repeated dispersion and centrifugation using 1,000 mM NaCl for three times. The carbonate minerals as impurity were also removed by dispersing in pH 5.0 sodium acetate buffer solution (Morgan solution). To check the exchangeable cation composition, the treated clay minerals were repeatedly dispersed and centrifuged in 1,000 mM NH_4Cl for four times. Finally, each treated clay mineral was ultrasonically dispersed in 10.0 mM NH_4Cl solution and centrifuged. By measuring the cation (Na^+ , K^+ , Mg^{2+} , and Ca^{2+}) concentrations in the solution, the exchangeable cation composition was evaluated. Each of the NH_4^+ -saturated clay minerals obtained by the above procedure was repeatedly dispersed and centrifuged in 1,000 mM NaNO_3 for five times. By measuring the NH_4^+ concentration in the solution, the CEC of each treated clay mineral was determined [25].

Adsorption experiment

For ^{226}Ra adsorption experiments, 0.10 and 1.00 g of the treated clay minerals were dispersed in 30 mL of 10.0, 100,

500, and 1,000 mM NaCl in 50 mL centrifugation tubes (Nalgene). In each system, 0.3 mL of ^{226}Ra stock solution ($3,200 \text{ dpm mL}^{-1}$ equivalent to $6.4 \times 10^{-6} \text{ mM}$) was added to realize an ^{226}Ra concentration of $6.3 \times 10^{-8} \text{ mM}$. According to the thermodynamic data [8], Ra^{2+} should be the dominant Ra species in the experimental solutions. In the adjustment of pH, an alkali (e.g., NaOH) was not added to prevent the contamination of extra cations other than H^+ . Alternatively, a pre-determined amount of 100 mM HCl was added to each solution in the presence of montmorillonite to adjust the pH to 5.0–5.5 to be the same pH range of the solution in the presence of kaolinite. Blank samples for each NaCl concentration without clay minerals were similarly prepared. After shaking the sample solutions (including the blank) using a mix rotor for 2 days at room temperature ($\sim 25^\circ\text{C}$), filtered ($0.45 \mu\text{m}$, DISMIC-25cs, cellulose acetate) supernatants were collected in 100-mL glass beakers after centrifugation. The solutions in the beakers were evaporated on a hot plate at 140°C . The ^{226}Ra adsorption experiment at a condition of 10.0 mM NaCl concentration in the presence of 1.00 g of montmorillonite was avoided, because filtration was virtually impossible owing to remaining clay particles in the supernatant after the centrifugation.

The retained ^{226}Ra in the 100-mL beaker after evaporation was re-dissolved using 2 mL of 100 mM HNO_3 and poured into a plastic cylindrical container (diameter: 22 mm; height: 45 mm) with a filter paper on the bottom of the container to absorb the solution. The solution in the plastic container was subsequently dried with the aid of an infrared lamp. Residual ^{226}Ra on the 100-mL beaker was again re-dissolved by 2 mL of 100 mM HNO_3 , poured into the plastic container, and dried by the above procedure. The re-dissolution (for 100-mL beaker) and drying (for plastic container) processes were repeated four times. Finally, the filter paper on the bottom of the plastic container was covered by a circular disk (diameter: 22 mm; thickness: 2 mm) and tightly sealed by an adhesion bond that filled the space between the disk and the wall of the container. The recovery of ^{226}Ra in the sample solutions through the above procedure was higher than 90 % regardless of the sample NaCl concentrations. After aging the plastic containers for at least three weeks, they were used for γ -ray spectrometric analyses using coaxial-type Ge detectors.

Analytical procedure

The γ -ray spectrometer was calibrated by the standards prepared in the same geometrical arrangement as the samples. The sample ^{226}Ra activities at 186 keV agreed

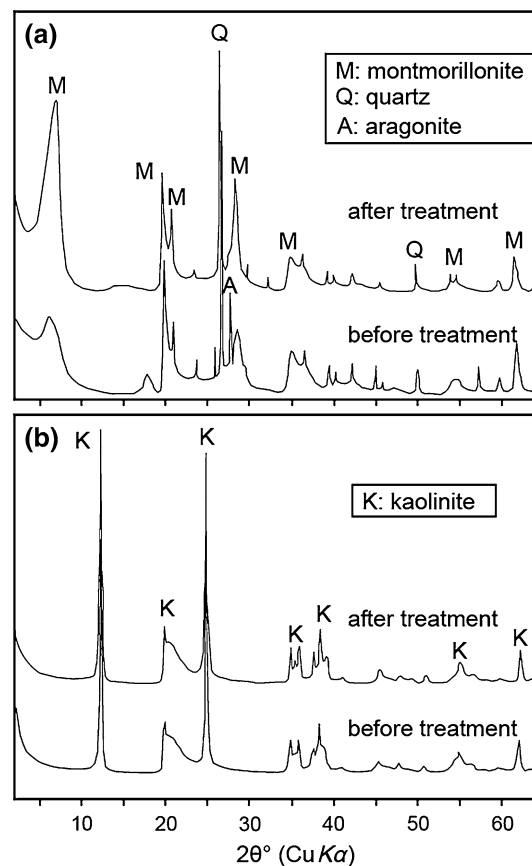


Fig. 2 X-ray powder diffraction profile for **a** montmorillonite and **b** kaolinite before and after Na^+ replacement for exchangeable cations and carbonate removal

with those measured via daughter nuclides, indicating that leakage of ^{222}Rn from the sample was negligible. The ^{226}Ra activity was obtained from its daughter (^{214}Pb) peak at 351.99 keV owing to its superior detectability. The γ -ray spectroscopy counting errors were usually lower than $\pm 1\%$. The relative standard deviation (RSD) of the measurements was about 0.06, judging from the fourfold blank sample measurements ($n = 4$). The adsorbed amounts of ^{226}Ra on the clay minerals were calculated by the difference between the ^{226}Ra concentrations of the sample and the blank. In the determination of the exchangeable cation composition and CEC for the clay minerals, the cation concentrations were measured by ion chromatography (Dionex, ICS-1,000). The RSD of the measurements were less than 0.011, 0.007, 0.060, 0.005, and 0.002 for Na^+ , NH_4^+ , K^+ , Mg^{2+} , and Ca^{2+} , respectively ($n = 2$). To assess purity of the clay minerals, X-ray powder diffraction (XRD) analyses (RIGAKU, RINT1200) with $\text{CuK}\alpha$ radiation at 40 kV and 30 mA were performed for original and treated (Na^+ -exchanged and carbonate-removed) montmorillonite and kaolinite.

Table 1 Exchangeable cation composition and CEC for treated clay minerals

	Exchangeable cation (mmol 100 g ⁻¹)				CEC (meq 100 g ⁻¹)
	Na ⁺	K ⁺	Mg ²⁺	Ca ²⁺	
Treated montmorillonite	73.8	D.L.	D.L.	D.L.	82.3
Treated kaolinite	4.9	8.7	D.L.	D.L.	3.1

Treated clay minerals were those in which exchangeable cations were exchanged with Na⁺, and carbonate minerals were removed via sodium acetate buffer solution at pH 5.0

CEC cation exchange capacity, D.L. detection limit

Results

Clay mineral characterization

In the XRD spectrum, aragonite (CaCO₃) in the original montmorillonite was not recognized in the treated montmorillonite (Fig. 2a). Quartz was found in both the original and the treated montmorillonite. The effect of quartz on the ²²⁶Ra adsorption experiment was neglected because quartz has negligible affinity with Ra compared to montmorillonite [5, 26]. No impure minerals were found in both the original and the treated kaolinite (Fig. 2b).

Table 1 summarizes the exchangeable cation compositions and CEC for the treated clay minerals. Only Na⁺ was detected as an exchangeable cation in the treated montmorillonite. The releasable Na⁺ amount (73.8 mmol 100 g⁻¹) was roughly consistent with CEC of the treated montmorillonite (82.3 mmol 100 g⁻¹). Similarly, the releasable amount of Na⁺ (4.9 mmol 100 g⁻¹) from the treated kaolinite was comparable to CEC of the treated kaolinite (3.1 mmol 100 g⁻¹). These observations signified successful Na⁺ exchange for exchangeable cations in the treated clay minerals. On the other hand, the releasable amount of K⁺ (8.7 mmol 100 g⁻¹) from the treated kaolinite was higher than its CEC, implying another source of K⁺ from cation exchangeable sites. The effect of released K⁺ from the treated kaolinite on the ²²⁶Ra adsorption experimental results was not taken into account, because Na⁺ concentrations in the experiment (≥10.0 mM) should have been higher than the released K⁺ concentrations in the experiment based on the releasable K⁺ amount (8.7 mmol 100 g⁻¹) of the treated kaolinite.

Adsorption experiment

Table 2 summarizes the percentage of dissolved ²²⁶Ra in the presence of the clay minerals and distribution coefficients (mL g⁻¹) of ²²⁶Ra. The dissolved percentage of ²²⁶Ra in the presence of both clay minerals (Fig. 3)

increased with the NaCl concentration. At the highest NaCl concentration (1,000 mM), the dissolved percentages of ²²⁶Ra were more than 80 % regardless of the clay minerals and solid/liquid ratios. The dissolved percentages of ²²⁶Ra were always higher in the presence of kaolinite than in the presence of montmorillonite, except at higher NaCl concentrations (≥500 mM). A lower solid/liquid ratio resulted in higher ²²⁶Ra dissolved percentages at a given NaCl concentration regardless of the clay minerals.

The distribution coefficients decreased with an increase in the NaCl concentration from the order of 10⁴ to 10⁰ (Fig. 4). They were higher for montmorillonite than for kaolinite at lower NaCl concentrations (≤100 mM), while the opposite trend emerged at higher NaCl concentrations. An increase in the solid/liquid ratio resulted in up to a five-fold decrease in the distribution coefficients at higher NaCl concentrations (≥500 mM).

Discussion

The distribution coefficient dependence on NaCl concentration was fitted by the function $D = \alpha Q^\beta$, where D is distribution coefficient (mL g⁻¹), Q is the NaCl concentration (mM), and α and β are fitting parameters. β represents the distribution coefficient dependence on NaCl concentration, with $\beta = -1$ indicating inversely proportional reduction of the distribution coefficient with an increase in NaCl concentration. Lower β values (<-1) signify more rapid reduction of the coefficient. Figure 4 shows the results of the fits with the optimized fitting parameters in the formula and square of the correlation coefficients (R^2). The β values were lower for montmorillonite (average -1.37) than for kaolinite (average -0.91), indicating more rapid reduction of the coefficient for montmorillonite with an increase in the NaCl concentration.

Webster et al. [27] developed a mathematical model to describe the dissolved ²²⁶Ra concentration dependence on salt concentration in the presence of sediment particles. This model assumes that the adsorption flux of salt and Ra (mol s⁻¹) is proportional to their concentrations (mol L⁻¹) and vacant adsorption site density of the adsorbent (mol m⁻²). The desorption flux of salt and Ra (mol s⁻¹) are proportional to their adsorbed concentrations (mol m⁻²) on the adsorbent. Finally, the vacant adsorption site density is inversely proportional to the salt concentration. The model predicts that inversely proportional reduction of the distribution coefficient emerges with the salt concentration elevation. Average β values (-0.91) near -1 in the case of kaolinite could support the validity of the model, while those (-1.37) in the case of montmorillonite were significantly lower than the model prediction ($\beta = -1$).

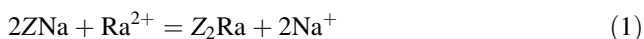
Table 2 Percentage of dissolved ²²⁶Ra in the presence of clay minerals and distribution coefficients of ²²⁶Ra

Samples	Solid/liquid ratio	NaCl concentration (mM)	Dissolved ²²⁶ Ra (%)	Distribution coefficient (mL g ⁻¹)
Montmorillonite	0.10 g/30 mL ⁻¹	10.0	3.0 ± 0.6	9,580 ± 1,820
		100	63.5 ± 0.8	170 ± 5
		500	88.9 ± 0.4	35.9 ± 1.6
		1,000	95.1 ± 0.5	15.6 ± 1.6
	1.00 g/30 mL ⁻¹	10.0	– ^a	–
		100	19.3 ± 2.0	126 ± 13
		500	57.6 ± 0.5	22.2 ± 0.3
		1,000	86.1 ± 0.5	4.84 ± 0.20
Kaolinite	0.10 g/30 mL ⁻¹	10.0	23.5 ± 1.3	959 ± 57
		100	89.1 ± 0.7	34.2 ± 2.4
		500	88.7 ± 0.4	38.0 ± 1.6
		1,000	92.2 ± 0.7	24.9 ± 2.2
	1.00 g/30 mL ⁻¹	10.0	4.2 ± 0.2	680 ± 25
		100	49.4 ± 0.3	30.8 ± 0.3
		500	88.8 ± 0.6	7.11 ± 0.30
		1,000	83.2 ± 0.8	6.03 ± 0.30

The errors are estimated from uncertainty of the measurements

^a The experiment was not performed in this condition owing to impossibility of the experimental solution for filtration because of remaining clay particles in the solution after centrifugation

Tachi et al. [23] described the Ra²⁺ adsorption on montmorillonite as



where Z is the cation adsorption site of montmorillonite. The equation leads to the different salinity dependence of

the Ra²⁺ distribution coefficient from the Webster’s model as shown below. Then, the derived salinity dependence is compared with the experimental results.

When an equilibrium state is established in Eq. (1), the following relationship is established [28]

$$K = \frac{(Z_2Ra)(Na^+)^2}{(ZNa)^2(Ra^{2+})} \tag{2}$$

where K is equilibrium constant, and the quantity in parentheses is activity of the species, which is approximated by molar concentration (M) in the following discussion. Almost all the cation exchange sites of the clay minerals are expected to be occupied by Na⁺, because clay minerals were Na⁺-saturated, the salt concentration were adjusted by NaCl, and Ra²⁺ concentration (6.3 × 10⁻⁸ mM) was extremely smaller than the Na⁺ concentrations (≥10 mM). Therefore, the cation exchange site concentration of the clay minerals occupied by Na⁺ (ZNa) should approximate the total cation exchange site concentration (Z)_t (M).

$$(Z)_t \cong (ZNa) \tag{3}$$

Equations (2) and (3) yield the following relationship.

$$\frac{(Z_2Ra)/(Z)_t}{(Ra^{2+})} = \frac{K(Z)_t}{(Na^+)^2} \tag{4}$$

The left-hand-side term expresses a quantity proportional to the distribution coefficient of Ra²⁺ with clay minerals, which is inversely proportional to the square of Na⁺ concentration in the right-hand-side term.

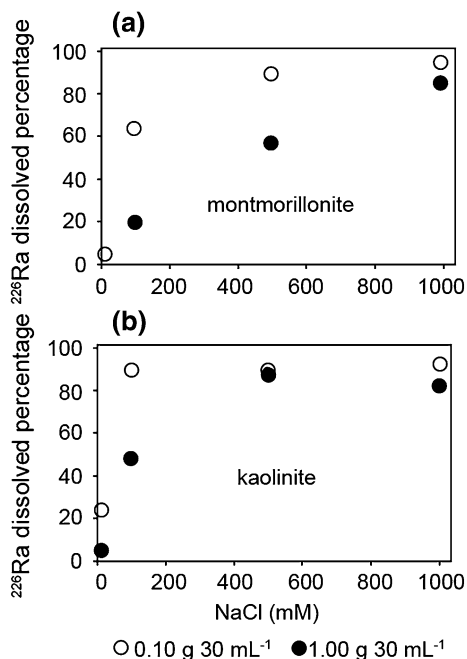


Fig. 3 ²²⁶Ra dissolved percentages in the presence of **a** montmorillonite and **b** kaolinite at 0.10 g/30 mL⁻¹ and 1.00 g/30 mL⁻¹ solid/liquid ratios as a function of NaCl concentration. Analytical errors arising from uncertainty of the measurements were within the size of the plots

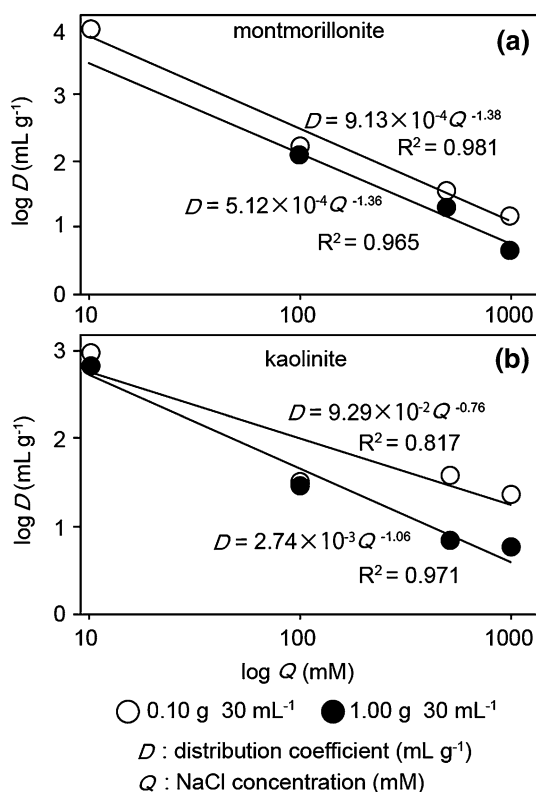


Fig. 4 ^{226}Ra distribution coefficient (D , mL g^{-1}) for **a** montmorillonite and **b** kaolinite at $0.10 \text{ g}/30 \text{ mL}^{-1}$ and $1.00 \text{ g}/30 \text{ mL}^{-1}$ solid/liquid ratios as a function of NaCl concentration (Q). Best fits of the function ($D = \alpha Q^\beta$) to the experimental results were also included. Optimized parameters (α , β) are shown on the graph in the function with the square of the correlation coefficients (R^2). Analytical errors arising from uncertainty of the measurements were within the size of the plots

The average β in case of montmorillonite (-1.37) was intermediate between -1 , as predicted in the model of Webster et al. [27], and -2 , as predicted from Eq. (4). The higher CEC of the montmorillonite than that of the kaolinite (Table 1) indicate higher negative charge density of the montmorillonite. The positive charge of a Ra^{2+} ion adsorbed on the montmorillonite should then be compensated by more negative charges (up to -2) than the case of the kaolinite. The situation should lead the adsorption mechanism of Ra^{2+} on montmorillonite to approach the Eq. (1) (complete charge compensation). This could be the reason for the lower value of β for the montmorillonite than that for the kaolinite.

Although distribution coefficient (mL g^{-1}) is not expected to be dependent on solid/liquid ratios [27], a negative correlation was observed between them in our experiments (Fig. 4, especially at NaCl concentrations $\geq 500 \text{ mM}$). This phenomenon could be explained by reduced mobility of clay particles, hence reactivity of those with ^{226}Ra , at higher clay particle and salt concentrations [29].

Conclusion

A positive correlation was observed between the dissolved ^{226}Ra and NaCl concentration in the presence of montmorillonite and kaolinite. Although CEC was considerably higher for montmorillonite ($82.3 \text{ mmol } 100 \text{ g}^{-1}$) than for kaolinite ($3.1 \text{ mmol } 100 \text{ g}^{-1}$), the distribution coefficients for montmorillonite became comparable to or lower than those for kaolinite at higher NaCl concentrations ($\geq 500 \text{ mM}$). The rapid decrease in the coefficient for montmorillonite with an increase in NaCl concentration was attributed to higher negative charge density (CEC) of montmorillonite, which leads the Ra^{2+} adsorption mechanism to approach charge-compensating ion exchange. It was concluded that CEC and relevant crystal structure of the clay minerals significantly influence salinity dependence of Ra adsorption on the clay minerals in natural groundwater.

Acknowledgments We thank M. Fuchizaki, Kanazawa University, for the XRD spectral measurements. T. Murakami, Kanazawa University, is acknowledged for valuable comments in the interpretation of the experimental results.

References

1. Gascoyne M (1989) High levels of uranium and radium in groundwaters at Canada's Underground Research Laboratory, Lac du Bonnet, Manitoba, Canada. *Appl Geochem* 4:577–591
2. Minster T, Ilani S, Kronfeld J, Even O, Godfrey-Smith DI (2004) Radium contamination in the Nizzana-1 water well, Negev Desert, Israel. *J Environ Radioact* 71:261–273
3. Vengosh A, Hirschfeld D, Vinson D, Dwyer G, Raanan H, Rimawi O, Al-Zoubi A, Akkawi E, Marie A, Haquin G, Zaarur S, Canor J (2009) High naturally occurring radioactivity in fossil groundwater from the Middle East. *Environ Sci Technol* 43:1769–1775
4. Vinson DS, Vengosh A, Hirschfeld D, Dwyer GS (2009) Relationships between radium and radon occurrence and hydrochemistry in fresh groundwater from fractured crystalline rocks, North Carolina (USA). *Chem Geol* 260:159–171
5. Ames LL, McGarrah JE, Walker BA (1983) Sorption of trace constituents from aqueous solutions onto secondary minerals. II. Radium. *Clay Clay Miner* 31:335–342
6. Chalupnik S, Michalik B, Wysocka M, Skubacz K, Mielnikow A (2001) Contamination of settling ponds and rivers as a result of discharge of radium-bearing waters from Polish coal mines. *J Environ Radioact* 54:85–98
7. Krishnaswami S, Graustein WC, Turekian KK (1982) Radium, thorium and radioactive lead isotopes in groundwaters: application to the in situ determination of adsorption-desorption rate constants and retardation factors. *Water Resour Res* 18:1633–1675
8. Langmuir D, Riese AC (1985) The thermodynamic properties of radium. *Geochim Cosmochim Acta* 49:1593–1601
9. Herczeg AL, Simpson HJ, Anderson RF, Trier RM, Mathieu GG, Deck BL (1988) Uranium and radium mobility in groundwaters and brines within the Delaware Basin, southeastern New Mexico, U.S.A. *Chem Geol (Isot Geosci Sect)* 72:181–196
10. Krishnaswami S, Bhushan R, Baskaran M (1991) Radium isotopes and ^{222}Rn in shallow brines, Kharaghoda (India). *Chem Geol (Isot Geosci Sect)* 87:125–136

11. Hidaka H, Horie K, Gauthier-Lafaye F (2007) Transport and selective uptake of radium into natural clay minerals. *Earth Planet Sci Lett* 264:167–176
12. Kraemer TF, Reid DF (1984) The occurrence and behavior of radium in saline formation water of the U.S. gulf coast region. *Chem Geol (Isot Geosc)* 2:153–174
13. Moise T, Starinsky A, Katz A, Kolodny Y (2000) Ra isotopes and Rn in brines and ground waters of the Jordan-Dead Sea Rift Valley: enrichment, retardation, and mixing. *Geochim Cosmochim Acta* 64:2371–2388
14. Sturchio NC, Banner JL, Binz CM, Heraty LB, Musgrove M (2001) Radium geochemistry of ground waters in Paleozoic carbonate aquifers, midcontinent, USA. *Appl Geochem* 16:109–122
15. Tomita J, Satake H, Sasaki K, Sakaguchi A, Inoue M, Hamajima Y, Yamamoto M (2009) Radium isotope in Na-Cl type saline waters from deep wells around coastal area in Ishikawa Prefecture, Japan. *J Hot Spring Sci* 58:241–255 (in Japanese with English abstract)
16. Tomita J, Satake H, Fukuyama T, Sasaki K, Sakaguchi A, Yamamoto M (2010) Radium geochemistry in Na-Cl type groundwater in Niigata Prefecture, Japan. *J Environ Radioact* 101:201–210
17. Dickson BL (1985) Radium isotopes in saline seepages, southwestern Yilgarn, Western Australia. *Geochim Cosmochim Acta* 49:361–368
18. Langmuir D (1997) *Aqueous environmental geochemistry*. Prentice Hall, Englewood Cliffs
19. Beneš P, Borovec Z, Strejc P (1985) Interaction of radium with freshwater sediments and their mineral components. II. Kaolinite and montmorillonite. *J Radioanal Nucl Chem* 89:339–351
20. Beneš P, Borovec Z, Strejc P (1986) Interaction of radium with freshwater sediments and their mineral components. III. Muscovite and feldspar. *J Radioanal Nucl Chem* 98:91–103
21. Wang RS, Chau ASY, Flu F, Cheng H, Nar P, Chen XM, Wu QY (1993) Studies on the adsorption and migration of radium in natural minerals. *J Radioanal Nucl Chem* 171:347–364
22. Komarneni S, Kozai N, Paulus WJ (2001) Superselective clay for radium uptake. *Nature* 410:771
23. Tachi Y, Shibutani T, Sato H, Yui M (2001) Experimental and modeling studies on sorption and diffusion of radium in bentonite. *J Contam Hydrol* 47:171–186
24. Velde B, Meunier A (2008) *The origin of clay minerals in soils and weathered rocks*. Springer, Berlin
25. Shirozu H (1988) *Introduction to clay mineralogy -fundamentals for clay science-*. Asakura, Tokyo
26. Beneš P, Strejc P, Lukavec Z (1984) Interaction of radium with freshwater sediments and their mineral components. *I J Radioanal Nucl Chem* 82:275–285
27. Webster IT, Hancock GJ, Murray AS (1995) Modelling the effect of salinity on radium desorption from sediments. *Geochim Cosmochim Acta* 59:2469–2476
28. Drever JI (1997) *The geochemistry of natural waters*, 3rd edn. Prentice Hall, Englewood Cliffs
29. Lagaly G (2006) In: Bergaya F, Theng BKG, Lagaly G (eds) *Handbook of clay science*. Elsevier, Oxford